Prediction of local mean power using 2-D ray-tracing-based propagation models

Y are the survivor sets defined earlier in Section IV-A. The resultant subsets are

$$F_{k,j}^{+} = \begin{cases} S_{k,j}^{+} \times Y & k = 1 \\ X \times S_{k,j}^{+} & k = 2 \end{cases}$$
$$F_{k,j}^{-} = \begin{cases} S_{k,j}^{-} \times Y & k = 1 \\ X \times S_{k,j}^{-} & k = 2. \end{cases} \quad (17)$$

For any pair of (k, j), the subsets $F_{k,j}^{+}$ and $F_{k,j}^{-}$ are both of size $32L$. Finally, by replacing the sets $D_{k,j}^{+}$ and $D_{k,j}^{-}$ in (15) by $F_{k,j}^{+}$ and $F_{k,j}^{-}$, we obtain the following reduced complexity MSD-DM receiver:

$$\Lambda_{k,j} = \ln\left[\frac{P_r(t_{k,j} = 1/\boldsymbol{R}_1, \boldsymbol{R}_2, \ldots, \boldsymbol{R}_N)}{P_r(t_{k,j} = 0/\boldsymbol{R}_1, \boldsymbol{R}_2, \ldots, \boldsymbol{R}_N)}\right]$$
$$\cong \max_{(c_1,\ldots,c_N)\in F_{k,j}^{+}} \left\{\left|\sum_{m=1}^{N} z_{m,c_m}\right|^2\right\} - \max_{(c_1,\ldots,c_N)\in F_{k,j}^{-}} \left\{\left|\sum_{m=1}^{N} z_{m,c_m}\right|^2\right\}. \quad (18)$$

Note that the reduction in complexity is approximately a factor of $64/L$.

Fig. 8 shows the simulated BER performance of the reduced-complexity MSD receiver in the AWGN channel. Compared to the original MSD receivers, the $L = 4$, $N = 2$ MSD-SM and the $L = 5$, $N = 2$ MSD-DM receivers only suffer a small performance degradation on the order of 0.05 dB. The complexity reduction, however, is significant.

V. Conclusion

In this paper, we propose to use multiple-symbol detection in orthogonal modulation systems. For uncoded systems, the MSD receiver provides the same asymptotic symbol error performance as the ideal coherent detector and is about 0.7 dB better than the conventional symbol-by-symbol detector. When applied to the CDMA IS-95 system, which is coded, the proposed MSD receivers are about 0.5 dB better than their conventional SBSD counterparts in both the AWGN and the fading channels. We also present in this paper reduced-complexity versions of the proposed MSD receivers. It was found that significant reduction in complexity can be achieved with only a small degradation in performance.

Although we only incorporated the MSD into the SM and DM receivers, the MSD technique can also be used in decision feedback receivers and soft-in/soft-out iterative decoding receivers to achieve performance enhancement.

Acknowledgment

The authors would like to thank the two reviewers for their comments and suggestions, which helped improve this paper significantly.

References

[1] A. J. Viterbi, A. M. Viterbi, and E. Zehavi, "Performance of power-controlled wideband terrestrial digital communication," *IEEE Trans. Commun.*, pp. 559–569, Apr. 1993.
[2] A. J. Viterbi, *CDMA Principles of Spread Spectrum Communication*. Reading, MA: Addison-Wesley, 1995.
[3] A. Viterbi and A. J. Viterbi, "Noncoherent receiver employing a dual-maxima metric generation process," U.S. Patent 5 442 627, June 1993.
[4] T. Frey and P. Schramm, "Concatenated coded spreading with coherent demodulation for DS-CDMA," in *Proc. IEEE VTC'98*, 1998, pp. 1910–1914.
[5] P. Schramm, "Comparison of attractive modulation schemes for the uplink in DS-CDMA systems," in *Proc. IEEE ICC'97*, 1997, pp. 1228–1232.
[6] D. Rabinowitz and E. Magana, "Decision feedback for IS-95 uplink frame decoding," *IEEE Trans. Veh. Technol.*, vol. 48, pp. 527–532, Mar. 1999.
[7] R. Herzog, J. Hagenauer, and A. Schmidbauer, "Soft-in/soft-out Hadamard despreader for iterative decoding in the IS-95(A) system," in *Proc. IEEE ICC'97*, 1997, pp. 1219–1222.
[8] D. Divsalar and M. K. Simon, "Multiple-symbol differential detection of MPSK," *IEEE Trans. Commun.*, vol. 38, pp. 300–308, Mar. 1990.
[9] J. G. Proakis, *Digital Communications*. New York: McGraw-Hill, 1983.

Prediction of Local Mean Power Using 2-D Ray-Tracing-Based Propagation Models

Yvo L. C. de Jong and Matti H. A. J. Herben

***Abstract*—A new method is presented for the computation of local mean power from individual multipath signals predicted by two-dimensional ray-tracing-based propagation models. This method is based on an expression for the spatial average of the received power, which takes into account the spatial correlation between signals. Numerical results for some simple test configurations show that application of the common method of simply adding the ray powers can result in considerable errors, while the new method remains accurate—at the cost of slightly increased computational complexity.**

I. Introduction

Ray-tracing-based propagation prediction models are becoming widely accepted as suitable tools for the planning of mobile radio networks in urban environments. Two-dimensional (2-D) ray-tracing models have been applied successfully for field prediction when transmitting and receiving heights are quite below the rooftops of surrounding buildings [1], [2], as is normally the case in urban microcells. These models account for all multipath rays between the base station and observation points lying in the horizontal plane through the base station, each ray undergoing (multiple) interactions with the urban environment, such as reflection and/or diffraction, up to a prespecified order. The received field at any observation point is then calculated by taking the sum of the individual complex ray amplitudes (e.g., [1] and [3]). The possible ray trajectories and associated complex amplitudes are usually determined for a set of discrete observation points, but the channel parameters computed from these predicted multipaths are assumed to be representative for an area around each observation point. The dimensions of such an observation area are typically on the order of several tens of wavelengths.

Probably the most important channel parameter is the local mean power, which is the total received signal intensity, averaged in space in order to remove small-scale fading. The predicted spatial distribution of the local mean power in a reception area around the base station antenna—appropriately subdivided into smaller observation areas

Manuscript received September 28, 1999; revised February 23, 2000. This work was supported by KPN Research, Leidschendam, The Netherlands.

The authors are with the Department of Electrical Engineering, Eindhoven University of Technology, Eindhoven 5600 MB The Netherlands (e-mail: y.l.c.d.jong@tue.nl).

Publisher Item Identifier S 0018-9545(01)03937-8.

(sometimes called *pixels*), the dimensions of which depend on the desired spatial resolution—can be used as the basis for the coverage and interference calculations required in the planning stage of cellular radio networks. An often used method to estimate the mean power for each observation area is to simply add the individual ray powers [1], [2], [4]. This method has been referred to as the sum of individual ray powers (SP) in [1]. In this paper, we present an alternative method, which is based on the spatial average (SA) of the received power over each pixel area but does not require ray tracing for more than one observation point per pixel. Unlike the SP method, the SA method provides a statistically valid approximation of the expected field strength at a random receiver position within a given observation area. Further, this method allows a fairer comparison to be made between propagation predictions and propagation measurement data obtained with a moving receiving antenna, in which the long-term fading component is usually also determined by spatial averaging—albeit in only one dimension.

II. Formulation

Consider the area S around the observation point O, which is assumed to be at the origin of a rectangular coordinate system (x, y); and assume that N rays are incident on O from the angles of arrival φ_n, $n = 1, 2, \ldots, N$ (see Fig. 1). Associated with each ray is a narrow-band signal with amplitude u_n and phase ϕ_n. If u_n and φ_n do not vary over the observation area S (plane wave assumption), the total received signal s can be evaluated at any point within S as

$$s(x, y) = \sum_{n=1}^{N} u_n \exp[jk(x \cos \varphi_n + y \sin \varphi_n) + j\phi_n] \qquad (1)$$

with k being the free-space wavenumber. The corresponding received power is

$$p(x, y) = |s(x, y)|^2. \qquad (2)$$

Both $s(x, y)$ and $p(x, y)$ are deterministic functions of the coordinates x and y and the known ray parameters u_n, ϕ_n, and φ_n.

The received power at a random observation point X in S obviously has a probabilistic nature, and it will be denoted by the random variable $P = p(X)$. Here, we assume that the (two-dimensional) random location variable X has a probability distribution $f_X(x, y)$ that is uniform in S. Under this assumption, the statistical mean $\overline{P}$ of the received power is identical to the received power averaged over S.

III. Computation of Local Mean Power

The mean power $\overline{P}$ in the observation area S can be found by integration of $p(x, y) f_X(x, y)$ over S, which gives

$$\overline{P} = \sum_{n=1}^{N} u_n^2 + 2 \sum_{m=1}^{N} \sum_{n<m} u_m u_n \mathrm{Re}\{\rho_{mn}\} \qquad (3)$$

where

$$\rho_{mn} = \iint_S \exp[jk(x \cos \varphi_m + y \sin \varphi_m) + j\phi_m] \times \exp[-jk(x \cos \varphi_n + y \sin \varphi_n) - j\phi_n] \times f_X(x, y)\, dx\, dy \qquad (4)$$

is a complex scalar that lies on or inside the unit circle and represents the spatial correlation between the mth and the nth multipath signal in S. When ρ_{mn} lies on the unit circle, the two signals are fully coherent.

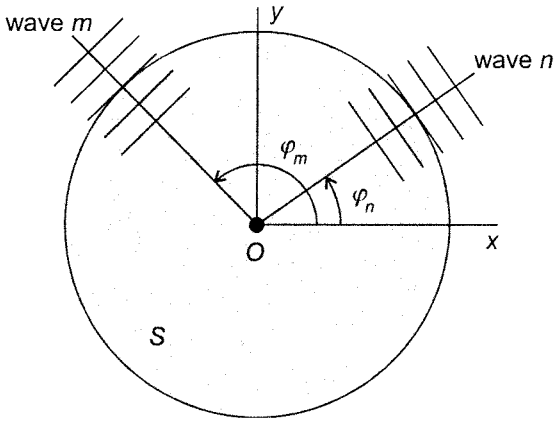

Fig. 1. Horizontal observation area S with incident multipath rays.

If ρ_{mn} lies inside the unit circle, the two signals are only partially correlated, while $\rho_{mn} = 0$ implies totally uncorrelated multipath signals.

For a rectangular observation area centered at O, with sides of lengths D_x and D_y aligned with the x and y axes, respectively, ρ_{mn} can be written as

$$\rho_{mn} = \frac{\sin[kD_x(\cos \varphi_m - \cos \varphi_n)/2]}{kD_x(\cos \varphi_m - \cos \varphi_n)/2} \times \frac{\sin[kD_y(\sin \varphi_m - \sin \varphi_n)/2]}{kD_y(\sin \varphi_m - \sin \varphi_n)/2} \exp[j(\phi_m - \phi_n)]. \qquad (5)$$

The predicted local mean power along a measurement trajectory can be obtained by locally orienting the (x, y) coordinate system with the x-axis parallel to the trajectory, making D_x equal to the averaging interval applied in the measurements; and letting $D_y \to 0$, so that the second factor in (5) vanishes. For a circular observation area of diameter D centered at O, ρ_{mn} becomes

$$\rho_{mn} = \frac{2J_1(kD \sin[(\varphi_m - \varphi_n)/2])}{kD \sin[(\varphi_m - \varphi_n)/2]} \exp[j(\phi_m - \phi_n)] \qquad (6)$$

where $J_1(\cdot)$ is the Bessel function of the first kind of order one. Finally, for the prediction of the mean power received along a horizontal circle centered at O with diameter D (ring-shaped observation domain), ρ_{mn} is given by

$$\rho_{mn} = J_0(kD \sin[(\varphi_m - \varphi_n)/2]) \exp[j(\phi_m - \phi_n)] \qquad (7)$$

where $J_0(\cdot)$ is the Bessel function of the first kind of order zero. Plots of the absolute correlation $|\rho_{12}|$ between two multipath signals, computed from (5)–(7), are shown in Fig. 2 as a function of the angular difference $\Delta\varphi = \varphi_2 - \varphi_1$, for $kD_x = kD_y = kD = 100$.

Equatino (3) simplifies for the specific cases in which all multipath signals are totally correlated or uncorrelated. For nearly uncorrelated multipath signals ($\rho_{mn} \simeq 0$, $m \neq n$), $\overline{P}$ can be approximated as the sum of the individual multipath signal powers, as in the SP method

$$\overline{P} \simeq \sum_{n=1}^{N} u_n^2. \qquad (8)$$

From (3) to (7), we see that the SP method is generally valid only if at least one of the dimensions of the observation domain is large in terms of the wavelength and all rays are sufficiently spaced in angle. If all multipath signals are almost completely correlated ($|\rho_{mn}| \simeq 1$, $m \neq n$), then $\mathrm{Re}\{\rho_{mn}\} \simeq \cos(\phi_m - \phi_n)$, and the local mean power is well approximated by the received power at the observation point O,

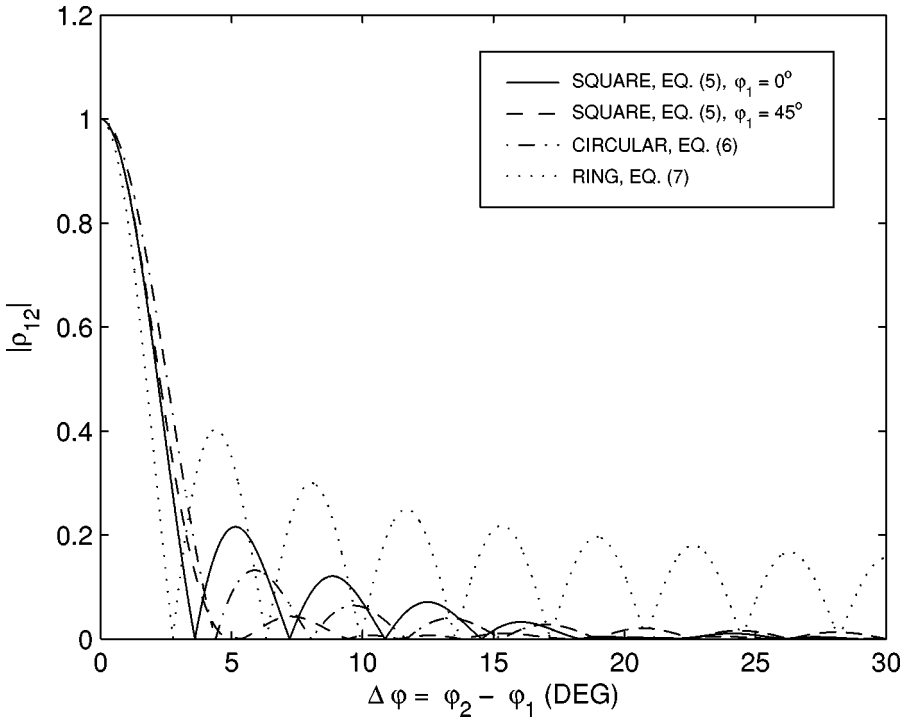

Fig. 2. Magnitude of the correlation coefficient versus the angular difference $\Delta\varphi = \varphi_2 - \varphi_1$ for a square observation area with $kD_x = kD_y = 100$, $\varphi_1 = 0°$; a square observation area with $kD_x = kD_y = 100$, $\varphi_1 = 45°$; a circular observation area with $kD = 100$; and a ring-shaped observation domain with $kD = 100$.

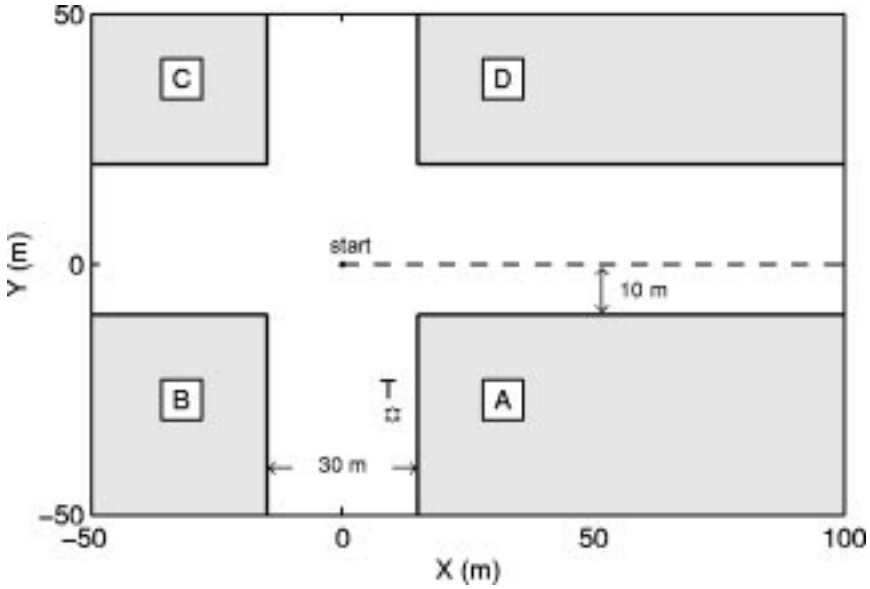

Fig. 3. Configuration of the test environment. Trajectory is indicated by the dashed line. "T" denotes the transmitter location.

which is calculated as the power of the sum of the individual multipath signals

$$\overline{P} \simeq \left| \sum_{n=1}^{N} u_n \ \exp(j\phi_n) \right|^2. \tag{9}$$

From (3) to (7), it is clear that this approximation is good as long as all dimensions of the observation area are small compared to the wavelength or the angular region from which all rays arrive is sufficiently small. In all other cases, in which one or more pairs of multipath signals are partially correlated, neither the SP method nor the received power at O forms a generally valid approximation of (3).

IV. Numerical Results

In this section, local mean power predictions computed using the SA method presented in this paper are compared with results obtained using the SP method in some simple test environments composed of one or more of the buildings marked as A–D in Fig. 3. Some of the configurations that can be composed in this way, such as the so-called two-corner and four-corner street intersections, have been investigated previously to study radio propagation around street corners [1], [2], [5]. In the present simulations, local mean power estimates are compared with each other and with the received power along the trajectory indicated in Fig. 3, and spatial distributions of

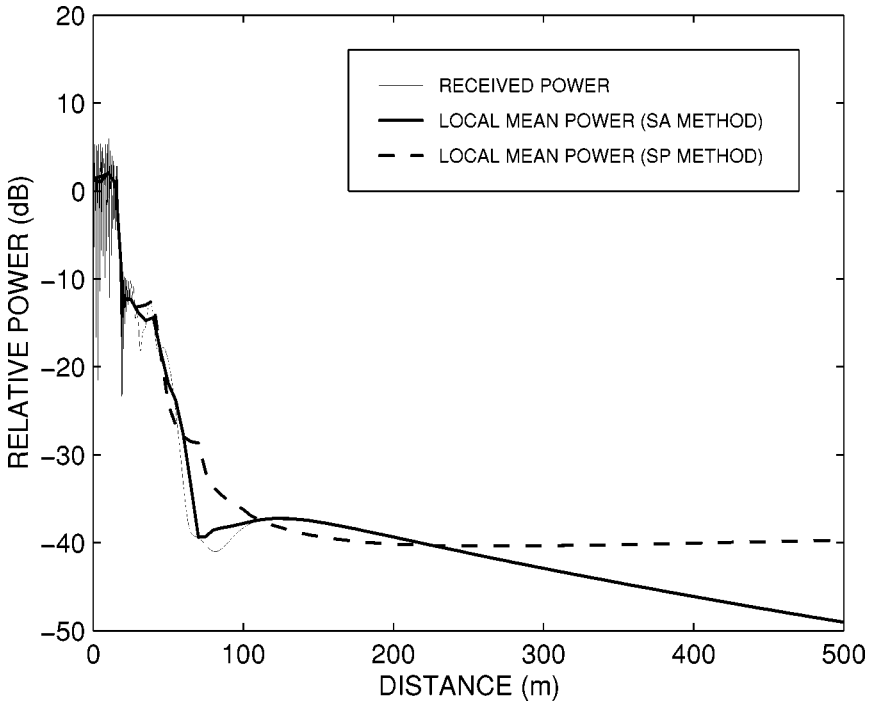

Fig. 4. Received power and local mean power estimates along the trajectory in configuration A + B (2-corner intersection). Local mean power estimates are computed using the SA method [(5), with $D_x = 5$ m and $D_y = 0$] and the SP method. Powers are relative to the free-space level.

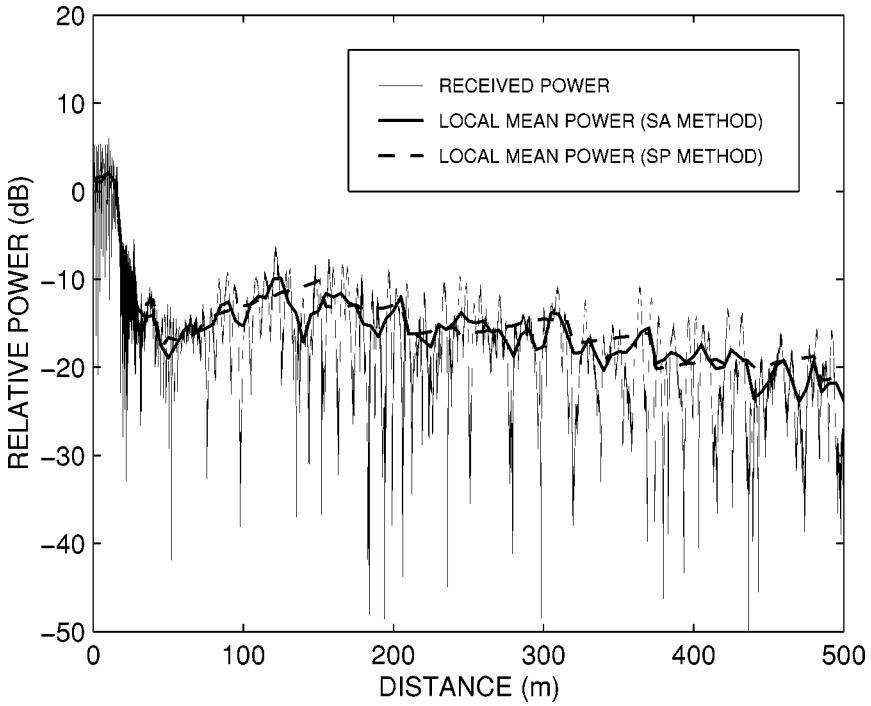

Fig. 5. Received power and local mean power estimates along the trajectory in configuration A + B + C + D (four-corner intersection). Local mean power estimates are computed using the SA method [(5), with $D_x = 5$ m and $D_y = 0$] and the SP method. Powers are relative to the free-space level.

the error made by the SP method (as compared with the SA method) are given for the complete coverage area. The transmitter is situated at a fixed location. Reflections up to tenth order and/or diffraction up to order two are taken into account, and the carrier frequency is 900 MHz. The diffraction contributions are computed using the diffraction coefficient for a wedge with impedance faces [6]. A relative permittivity of $\epsilon_r = 5.3$ and zero conductivity, corresponding to dry brick, are selected for the buildings.

Figs. 4 and 5 show the predicted received power and the local mean power estimates along the trajectory, evaluated using the SP method and the SA method, for the configurations consisting of buildings A + B (2-corner intersection) and buildings A + B + C + D (four-corner intersection), respectively. The received power is computed every 5 cm, while the local mean power estimates are evaluated every 5 m. For the SA method, a 5-m averaging interval [(5), with $D_x = 5$ m, $D_y = 0$] is applied. In the two-corner intersection case of Fig. 4, the received

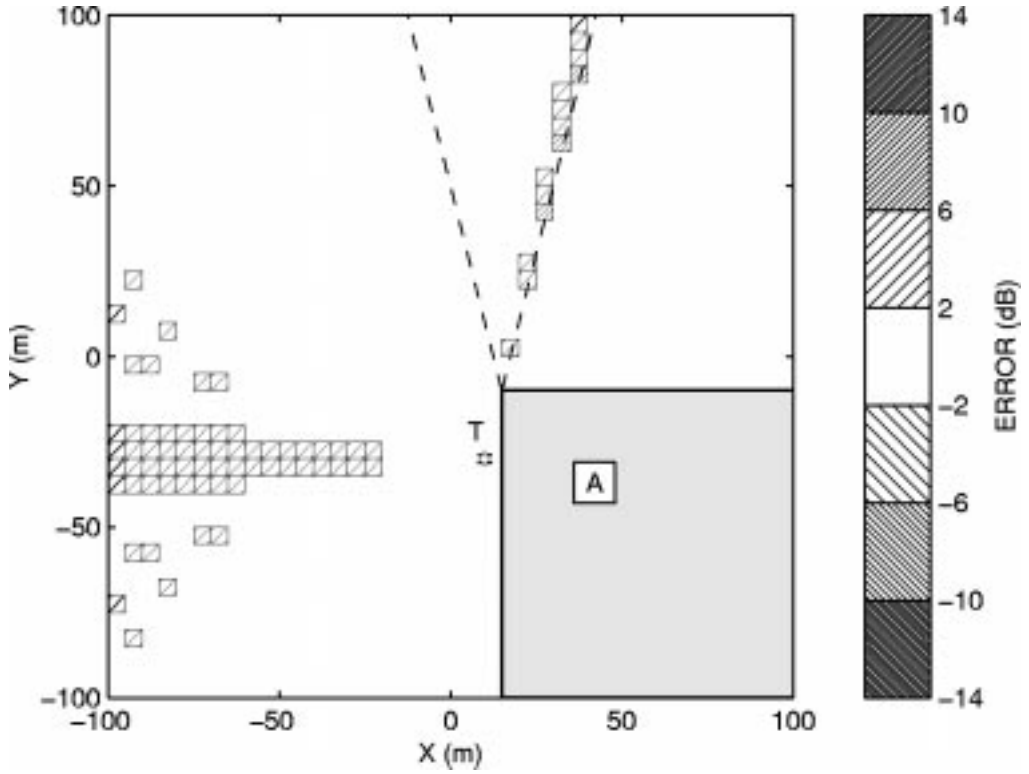

Fig. 6. Spatial distribution of the SP estimation error (relative to the SA method) for configuration A only (one-corner intersection). $D_x = D_y = 5$ m. "T" denotes the transmitter location. Dashed lines indicate the shadow and reflection boundaries of the direct ray.

power shows rapid fluctuations at distances close to the transmitter. As desired, the local mean power, estimated by either the SA or the SP method, does not follow these small-scale fluctuations. At larger distances from the transmitter, the SP method no longer accurately predicts the local mean power, whereas the SA method provides a good approximation at all distances from the transmitter. The error made by the SP method amounts to 10 dB at 500 m from the transmitter. In the four-corner intersection case of Fig. 5, on the other hand, the received power shows fast fluctuations along the entire 500 m trajectory, and both the SA and SP methods provide good estimations of the true local mean power.

A physical explanation for the observations made above can be given after considering the spatial distribution of the error made by applying the SP method, as compared with the SA method. Fig. 6 shows the error distribution for the configuration composed of building A only (one-corner intersection). The largest errors, ranging up to 7 dB, are found near the shadow boundary of the incident field. In this region, the first Fresnel zone of the direct wave is partially obstructed by building A, which is accounted for by ray-based diffraction theory through destructive interference with the wave diffracted from the corner of building A. Using the SP method, however, the power of this diffraction contribution is *added* to the power of the direct wave, which results in an overestimation of the local mean power. The SA method handles the contribution of the diffracted ray signal to the local mean power in a correct manner, by taking into account its high correlation with the "direct" signal. In the considered configuration, equally large errors do not occur near the reflection boundary, because the field in this region is dominated by the direct wave. Smaller but significant errors occur in other regions where the signals associated with the direct wave and the reflection from the wall behind the transmitter become strongly correlated.

Similar plots of the error distributions for the configurations A + B and A + B + C + D are shown in Figs. 7 and 8. Instead of two, there are now many shadow boundaries, each one associated with one of the many multipath waves reflected and/or diffracted between the buildings. For the two-corner intersection of Fig. 7, this results in considerable errors in large parts of the coverage area, as was also observed from Fig. 4. On the other hand, in the four-corner intersection configuration of Fig. 8, the diffraction contributions are dominated by multiple reflections in the street canyons formed by all four buildings, and these waves impinge on the receiver from a relatively wide angular region. The associated multipath signals therefore have low correlation, so that in this case, the SP method provides a good approximation of the local mean power in most of the coverage area, including the trajectory of Fig. 3.

V. Conclusions and Discussion

In this paper, we have proposed an accurate method for determining local mean power using 2-D ray-tracing-based propagation prediction models. This method, described by (3)–(7), automatically reduces to the commonly used SP method for uncorrelated multipath signals, but, unlike the SP method, remains valid for correlated signals, i.e., for rays arriving at the receiver from a narrow angular region. Although it is based on the spatial average of the received power, this method does not require the calculation of the received power at many discrete points within each observation area or interval, as is the case in [1].

Numerical results for some simple test configurations show that application of the SP method can result in considerable estimation errors, while the new SA method remains accurate in all cases. They further indicate that poor performance of the SP method occurs particularly near the shadow boundaries associated with diffracted rays. In the most complex test environment considered in this paper (Fig. 8), the SP method was shown to give results similar to the new SA method. Although this may suggest that the conventional power sum gives a sufficiently good approximation of the local mean power in complex

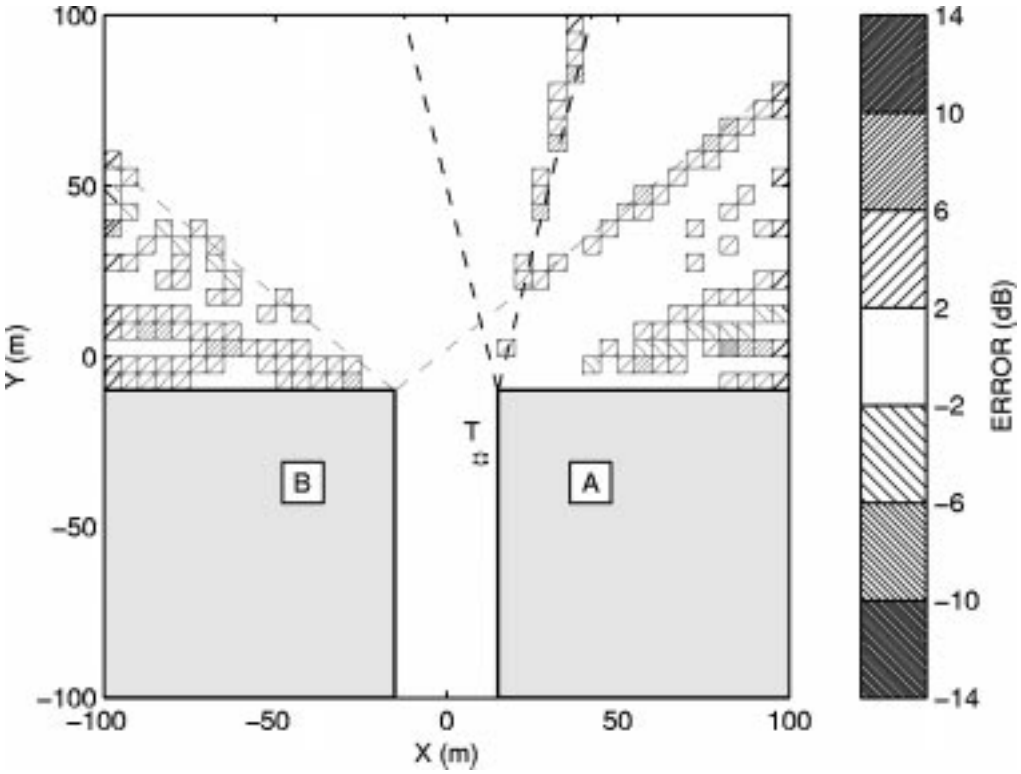

Fig. 7. Spatial distribution of the SP estimation error (relative to the SA method) for configuration A + B (2-corner intersection). $D_x = D_y = 5$ m. "T" denotes the transmitter location. Dashed lines indicate the shadow and reflection boundaries of the direct ray.

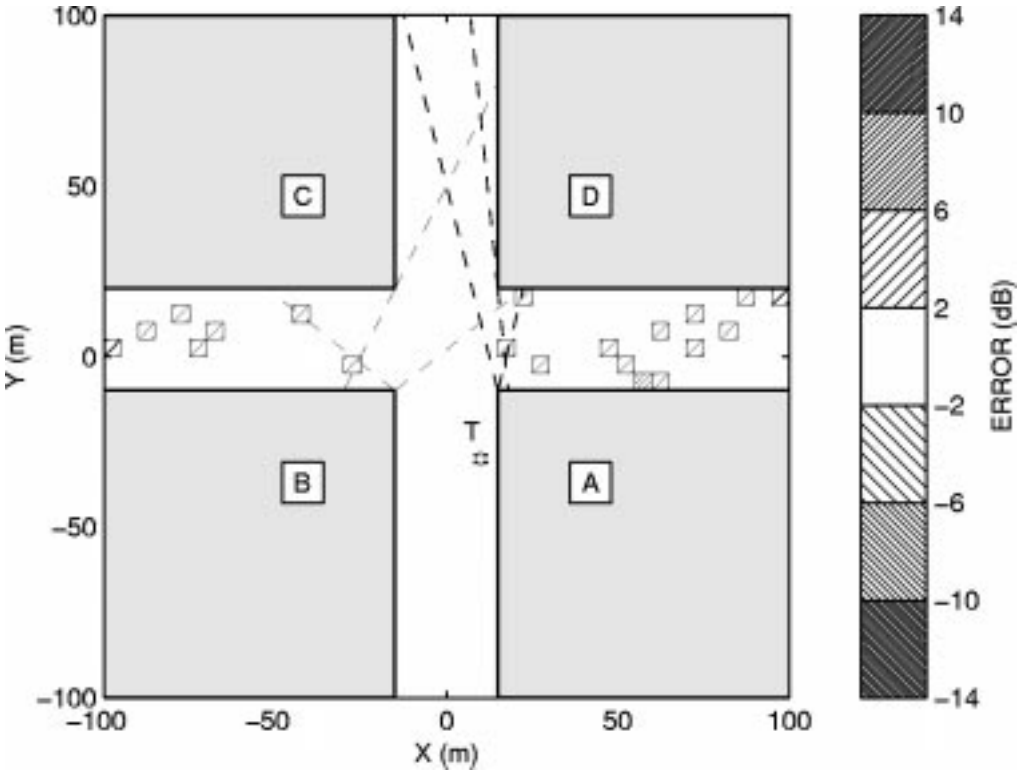

Fig. 8. Spatial distribution of the SP estimation error (relative to the SA method) for configuration A + B + C + D (4-corner intersection). $D_x = D_y = 5$ m. "T" denotes the transmitter location. Dashed lines indicate the shadow and reflection boundaries of the direct ray.

environments, it is hard or even impossible to say in general for what building configurations and/or in which parts of a reception area the SP method provides accurate results.

The presented method can be extended to three-dimensional ray-tracing models in a straightforward manner. Computation of the local mean power then involves an integration of the received power over

a volume around each observation point, and the correlation between multipath signal pairs will depend on the angular spacing of the corresponding rays in both azimuth and elevation.

REFERENCES

[1] V. Erceg, A. J. Rustako, and R. S. Roman, "Diffraction around corners and its effects on the microcell coverage area in urban and suburban environments at 900 MHz, 2 GHz, and 6 GHz," *IEEE Trans. Veh. Technol.*, vol. 43, no. 3, pp. 762–766, 1994.

[2] K. Rizk, J.-F. Wagen, and F. Gardiol, "Two-dimensional ray tracing modeling for propagation prediction in microcellular environments," *IEEE Trans. Veh. Technol.*, vol. 46, no. 2, pp. 508–518, 1997.

[3] G. Lampard and T. Vu-Dinh, "The effect of terrain on radio propagation in urban microcells," *IEEE Trans. Veh. Technol.*, vol. 42, no. 3, pp. 314–317, 1993.

[4] S.-C. Kim, B. J. Guarino, T. M. Willis, V. Erceg, S. J. Fortune, R. A. Valenzuela, L. W. Thomas, J. Ling, and J. D. Moore, "Radio propagation measurements and prediction using three-dimensional ray tracing in urban environments at 908 MHz and 1.9 GHz," *IEEE Trans. Veh. Technol.*, vol. 48, no. 3, pp. 931–946, 1999.

[5] J.-F. Wagen and K. Rizk, "Ray tracing based prediction of impulse responses in urban microcells," in *Proc. VTC'94*, Stockholm, Sweden, 1994, pp. 210–214.

[6] R. Tiberio, G. Pelosi, and G. Manara, "A uniform GTD formulation for the diffraction by a wedge with impedance faces," *IEEE Trans. Antennas Propagat.*, vol. 33, no. 8, pp. 867–873, 1985.

Corrections to "The Path Loss Model for UMTS Vehicular Test Environment"

José M. Hernando and Luis Mendo

I. INTRODUCTION

Some inaccuracies have been found in the path loss model that is proposed by ETSI [1, Section 1.8.1.3] for the vehicular test environment of the Universal Mobile Telecommunications System (UMTS). Since this propagation model is being used for simulation and system evaluation purposes, it is important to point out this fact.

II. CORRECTIONS

We first note some minor typographical errors.

1) In the first equation in [1, p. 65], d should be replaced by the variable R, representing the distance between the transmitter and receiver.
2) In the second and third equations on the same page, d should be replaced by b, the building spacing.

The effect of base-station antenna height Δh_b on the path-loss slope is claimed in [1] to have been taken from [2] . However, from [2, Fig. 9(b)], a slope variation of the form $4 - 8 \cdot 10^{-2}\Delta h_b$ is obtained. The third equation in [1, p. 65] should then be written as

$$L = -10\log_{10}\left[\left(\frac{\lambda}{4\pi R}\right)^2\right] - 10\log_{10}\left[\frac{\lambda}{2\pi^2 r}\left(\frac{1}{\theta} - \frac{1}{2\pi+\theta}\right)^2\right] - 10\log_{10}\left[2.35^2\left(\Delta h_b\sqrt{\frac{d}{\lambda}}\right)^{1.8}/R^{2(1-4\cdot 10^{-2}\Delta h_b)}\right]. \quad (1)$$

Moreover, it should be noted that the mentioned figure in [2] has been obtained from measurements in suburban areas, and therefore it may not give accurate results for urban environments.

Substitution of the proposed values $\Delta h_m = 10.5$ m, $x = 15$ m, and $d = 80$ m into (1) yields

$$L = -32.3 + 21\log_{10} f(\text{MHz}) - 18\log_{10}\Delta h_b(\text{m}) + 40\log_{10} R(\text{m})\left[1 - 2\cdot 10^{-2}\Delta h_b(\text{m})\right]. \quad (2)$$

Inserting a conversion factor to express R in kilometers, we obtain

$$L = 87.7 - 2.4\Delta h_b(\text{m}) + 21\log_{10} f(\text{MHz}) - 18\log_{10}\Delta h_b(\text{m}) + 40\left[1 - 2\cdot 10^{-2}\Delta h_b(\text{m})\right]\log_{10} R(\text{km}). \quad (3)$$

Therefore, the sixth equation of [1, p. 65] is not correct and should be replaced by the (3) above.

REFERENCES

[1] *Universal Mobile Telecommunications System; Selection Procedures for the Choice of Radio Transmission Technologies of the UMTS (UMTS 30.03 version 3.2.0)*: European Telecommunications Standards Institute, 1998.

[2] H. H. Xia, H. L. Bertoni, L. R. Maciel, A. Lindsay-Stewart, and R. Rowe, "Microcellular propagation characteristics for personal communications in urban and suburban environments," *IEEE Trans. Veh. Technol.*, vol. 43, pp. 743–752, Aug. 1994.

Manuscript received January 25, 2000; revised April 18, 2000.

The authors are with the Departamento de Señales, Sistemas y Radiocomunicaciones, Universidad Politécnica de Madrid, Madrid 28040 Spain.

Publisher Item Identifier S 0018-9545(01)03225-X.

Comments on "A New Theoretical Model for the Prediction of Rapid Fading Variations in an Indoor Environment"

Ali Abdi

In this paper,[1] a new distribution, named POCA, was introduced for modeling envelope fluctuations due to fast fading in indoor environments. The main motivation has been the small number of scatterers in those environments, which makes the central limit theorem invalid for in-phase and quadrature components. Hence they are no

Manuscript received January 14, 1999; revised September 15, 1999. This work was supported in part by the National Science Foundation under Wireless Initiative Program Grant 9979443.

The author is with the Department of Electrical and Computer Engineering, University of Minnesota, Minneapolis, Minnesota, 55455 USA.

Publisher Item Identifier S 0018-9545(01)03224-8.

[1]D. S. Polydorou and C. N. Capsalis, *IEEE Trans. Veh. Technol.*, vol. 46, pp. 748–754, 1997.